BIOORGANIC CHEMISTRY 14, 55–69 (1986)

The Crystal and Molecular Structure of Quercetin: A Biologically Active and Naturally Occurring Flavonoid

MIRIAM ROSSI,*,†,[1] LORI F. RICKLES,† AND WENDY A. HALPIN*

*Department of Chemistry, Vassar College, Poughkeepsie, New York 12601 and †The Institute for Cancer Research, Philadelphia, Pennsylvania 19111

Received May 20, 1985

The crystal and molecular structure of quercetin, one of the bioflavonoids found in plants, is described. The structure is of interest because of the variety of biological systems affected by it. It is known to be an antitumor agent and to exhibit antiallergenic and anti-inflammatory activity. it is an antioxidant and a cardiostimulant. These biological functions are governed by a number of enzymes and so quercetin's interactions with these enzymes are well studied. Crystals suitable for X-ray diffraction were difficult to obtain. Crystal data are as follows: a = 13.060(5), b = 16.564(7), c = 3.725(2) Å, α = 92.05(4), β = 94.39(3), γ = 120.55(3), V = 689.4(5) Å^3, z = 2, space group $P\bar{1}$, D_c = 1.63 g cm^{-3}, D_m = 1.69(1) g cm^{-3}. Quercetin crystallizes with two waters of crystallization that participate in an extended hydrogen bonding network through the crystal lattice. There are intramolecular hydrogen bonds between two hydroxyl groups and the exocyclic oxygen, O4. Quercetin, in the crystal structure, exists as hydrogen-bonded dimers packing almost perpendicular to c. These dimers form a two-dimensional net, mostly in the ab plane, connected via water molecules. Additionally, the waters provide for hydrogen bonding in the z direction. The exocyclic oxygen appears to be the focal point of cohesive forces in the crystal structure. Its electron-withdrawing effects are stabilized by the high degree of hydrogen bonding. This, in turn, leads the exocyclic phenyl ring to exist in an almost planar conformation with respect to the rest of the molecule. The torsion angle between the phenyl ring and the pyrone ring is only 7°. As expected, from an analysis of the atomic charges, it is clear that quercetin has more polar groups than similar flavonoid compounds. Comparison with these structures is made.

INTRODUCTION

Flavonoids are a class of compounds commonly found in plants. They are all derivatives of the parent compound, flavone (**I**) (Scheme 1). These compounds, together with synthetic analogs, are biologically active in a variety of ways: they are inhibitors of carcinogenesis; they exhibit anti-inflammatory and antiallergenic activity; some are mutagenic (although not carcinogenic); they are antioxidants and have shown cardiostimulant activity (*1*). As substrates, inhibitors, and inducers, they interact with a variety of enzyme systems (*2–10*).

Quercetin (**II**) is a naturally occurring flavonoid which is ubiquitous in the human diet. It is found in many fruits and vegetables and is also ingested from tea, coffee, cocoa, wine, beer, and vinegar (*1*). The catabolism of flavonoids by intesti-

[1] To whom correspondence should be addressed.

0045-2068/86 $3.00

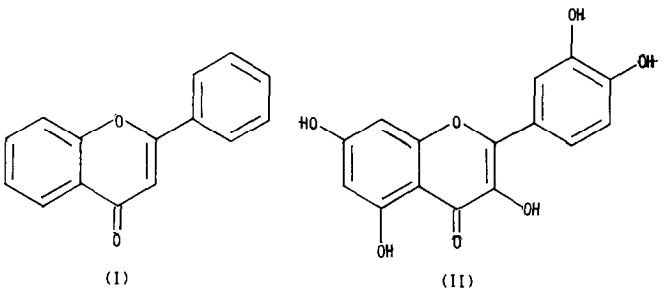

SCHEME 1.

nal microorganisms yields a variety of phenolic acids and phloroglucinol, which are usually nontoxic at these small concentrations (*11*). Quercetin is mutagenic, but apparently not carcinogenic (*12*) [apart from one report (*13*)]. It interacts in an inhibitory way with a number of seemingly disparate enzyme systems. Much of the work reported on quercetin consists of studies with regard to its antitumor activities; these include its inhibition of the cytochrome *P*-450 isozyme specific for polycyclic aromatic hydrocarbon metabolism.

The cytochrome *P*-450 enzyme system is inducible and is made up of two proteins in a lipid fraction: NADPH cytochrome *P*-450 reductase and a particular isozyme of cytochrome *P*-450 that is a mixed-function oxidase (*14*). The reductase catalyzes transfer of two electrons from NADPH to the cytochrome *P*-450 isozyme in two steps. These reduce the heme iron found at the active site from an Fe(III) to an Fe(II) oxidation state (the active form). The oxidase uses molecular oxygen as the oxidizing agent to catalyze the hydroxylation reactions. As many as ten different chemical oxidation reactions are catalyzed by these proteins. Each of the isozymes catalyzes position-specific hydroxylations. Flavonoids, including quercetin, have been shown to be potent inhibitors of the cytochrome *P*-450 system, particularly 7,8-benzoflavone (*15*), a synthetic flavone. Some studies have determined that quercetin actually inhibits NADPH cytochrome *P*-450 reductase (*16*). Furthermore, Huang and co-workers have found that quercetin interacts covalently with the "ultimate carcinogen" of benzo[*a*]pyrene, (±)-7β,8α-dihydroxy-9α,10α-epoxy-7,8,9,10-tetrahydrobenz[*a*]pyrene (*17*). This complex is nontoxic and is eliminated.

Quercetin inhibits tumor growth and there is experimental evidence for a number of mechanisms. It is known that tumor cells have a high rate of aerobic glycolysis due to enhanced ATPase activity (*18*). ATPase enzyme complexes direct the Na^+/K^+ pump and, from hydrolysis of ATP, produce ADP and P_i which are required for glycolysis. Quercetin is known to inhibit several adenosine triphosphatases involved in membrane transport (*7, 19*). The high rate of aerobic glycolysis in tumor cells produces large amounts of lactate. Quercetin causes intracellular lactate retention, thus lowering the cellular pH (*20*). Cells then become more susceptible to the cytotoxic effect of hyperthermia (*21*). Other reports of tumor suppression by quercetin ascribe this effect to the inhibition of lipoxygenase (*6*) and of a cAMP-independent protein kinase (*5, 22*). Lipoxygenase prod-

ucts stimulate production of ornithine decarboxylase and seem to be necessary for tumor promotion (*6*).

Several of quercetin's activities relate to Ca^{2+} movement in the cell: It inhibits histamine release (*23, 24*), Ca^{2+} transport across the membrane (*25, 26*), cyclic nucleotide phosphodiesterases (*4*), calmodulin (*27*), human platelet aggregation (*28*), leukocyte respiration (*29*), and prostaglandin synthesis (*30*). Quercetin inhibition of aldose reductase (*9, 31*) is of interest because of its function in a number of diabetic complications. Aldose reductase reduces hexose sugars to sugar alcohols. Flavonoids appear to be ascorbic acid synergists (*32*) and their antioxidant properties are due primarily to the many hydroxyl groups (*33*). Quercetin inhibits transcription by interaction with an RNA polymerase (*34*). It is a copper chelator; in this capacity it is a potent hyaluronidase inhibitor (*35*).

Because of the diversity of its functions in vivo, the study of the molecular structure of quercetin by single crystal x-ray analysis was undertaken to provide data to explore its mechanism of action. The results of this study are compared with those obtained from previously determined flavonoid compounds.

EXPERIMENTAL

Quercetin dihydrate was obtained from the Aldrich Chemical Company. A variety of crystallization techniques were employed but suitable crystals were very difficult to obtain. The best ones were prepared by evaporation of an aqueous ethanol solution; most were small, yellow, and twinned prisms. Initial Weissenberg photographs were taken to characterize the crystal and determine the suitability of the crystal quality. After many attempts, a single crystal of sufficient quality to warrant data collection was finally chosen. That is, the photographic diffraction spots were single and of reasonable intensity. Crystal data are given in Table 1. Since no mirror symmetry was evident in oscillation or subsequent upper level photographs, the space group was assumed to be $P\bar{1}$. Three-dimensional X-ray intensity data were collected using a crystal of size $0.15 \times 0.10 \times 0.07$ mm on a Nicolet P21 automated diffractometer with the θ–2θ scan technique and Cu$K\alpha$ radiation (using a highly oriented graphite crystal monochromator). Individual scan speeds were determined by a rapid scan at the position of the calculated Bragg peak and the rate of scanning varied from 2.0 deg min^{-1} (less than 50 counts during the rapid scan) to 29.3 deg min^{-1} (more than 500 counts during the rapid scan). Three reflections were routinely monitored at intervals of 100 reflections; these standard reflections showed little fluctuation in their intensity during the data collection (2.0 to 3.5%). No decay correction was made on the resulting data. A total of 2589 reflections were scanned in the range $(\sin\theta/\lambda) = 0.04$ to 0.61 $Å^{-1}$ ($2\theta = 138$), of which 1775 had $(I) > 2.5\sigma(I)$, where $\sigma(I)$ was derived from counting statistics. Values of $\sigma(F)$ were determined as $\sigma(F) = (F/2)\{[\sigma^2(I)/I^2] + \delta^2\}^{1/2}$ where δ is an instrumental uncertainty determined from the variation of the measured intensities of three periodically monitored standard reflections ($\delta = 0.030$). The data and their associated standard deviations were converted to structure

TABLE 1

CRYSTAL DATA FOR QUERCETIN DIHYDRATE
($C_{15}H_{10}O_7 \cdot 2H_2O$)

M_r	338.27	Space group	$P\bar{1}$
a	13.060(5)	Temperature	25°C
b	16.564(7)	D_c	1.63 g cm^{-3}
c	3.725(2) Å	D_m	1.69(1) g cm^{-3}
α	92.05(4)	$F(000)$	352
β	94.39(3)	$\mu(CuK\alpha)$	12.00 cm^{-1}
γ	120.55(3)°	λ	1.5418 Å
V	689.4(5) Å^3	$(\sin\theta)/\lambda_{max}$	0.61($2\theta_{max}$ = 138°)
z	2		

amplitudes by application of Lorentz and polarization factors. No absorption correction was made.

The structure was solved by direct methods using SHELX76 (*36*) and was revealed as all heavy atoms, including the two solvent (water) molecules. Isotropic, then anisotropic, refinement of all heavy atoms reduced the R value to 11.8 for the observed data. The quantity minimized in the least-squares calculations was $\Sigma w||F_0| - |F_c||^2$. The weights of the reflections, w, used during the refinement were $1/\sigma^2$ with zero weight for those reflections below the threshold value. All hydrogen atoms except for water hydrogens were located from a difference map and their inclusion reduced the R value ($R = \Sigma||F_0| - |F_c||/|F_0|$) to 10.7. The structure was refined further by full-matrix methods, keeping the hydrogens fixed with isotropic temperature factors set equal to the atoms with which they were bonded. The final residuals were $R = 9.5$, weighted $R = 10.4$. Further refinement of the structure was not possible. At this point, several attempts were made to determine the cause of the discrepancy between the observed and calculated structure factors. Upon examination of the data, it was clear that there was no secondary extinction affecting it. Difference Fourier methods were then used. The structure was placed in space group $P1$ but a difference Fourier synthesis revealed the second molecule to be centrosymmetrically related to the first indicating $P\bar{1}$ to be the correct space group. Removal of the oxygen atoms from the solvent water molecules as well as the diol oxygens to which they are hydrogen bonded simply resulted in the highest electron density peaks being identical to these atomic positions. A final difference Fourier map with all heavy atoms (including solvent water oxygens) and all hydrogen atoms except for those associated with the solvent after the last cycle of least squares resulted in the highest peak being equal to 0.9 Å^{-3}. These peaks were in the vicinity of the solvent molecules but could not be resolved into discrete hydrogen atom positions and any inclusion of these peaks with partial occupancy did nothing to help the agreement between the model and the data.

Computer programs were SHELX76 (*36*) and locally written programs, including those for plotting and graphics (on a Vector-General display monitor) (*37*). The

TABLE 2

REFINED ATOMIC PARAMETERS OF QUERCETIN

Atom	*x*	*y*	*z*	B_{11}	B_{22}	B_{33}	B_{12}	B_{13}	B_{23}
C(2)	0.5406(5)	0.2941(5)	0.523(2)	1.7(2)	1.8(2)	2.5(3)	1.1(2)	−0.5(2)	0.1(2)
C(3)	0.6440(5)	0.3775(5)	0.609(2)	1.7(2)	1.8(2)	3.0(3)	1.2(2)	−0.6(2)	0.4(2)
C(4)	0.7469(5)	0.3805(5)	0.801(2)	1.7(2)	1.7(2)	2.4(3)	0.9(2)	−0.6(2)	−0.2(2)
C(5)	0.8299(5)	0.2853(5)	1.051(2)	1.2(2)	2.0(2)	3.1(3)	0.7(2)	−0.4(2)	0.4(2)
C(6)	0.8172(5)	0.2011(5)	1.118(2)	1.6(2)	2.3(2)	4.1(4)	1.4(3)	−0.6(2)	0.5(3)
C(7)	0.7078(5)	0.1189(5)	1.002(2)	2.1(2)	1.8(2)	3.7(4)	1.3(2)	−0.1(2)	0.7(3)
C(8)	0.6111(5)	0.1211(5)	0.833(2)	1.9(2)	1.7(2)	3.0(3)	1.0(2)	−0.7(2)	0.1(2)
C(9)	0.6280(5)	0.2094(5)	0.768(2)	1.6(2)	2.0(2)	2.2(3)	1.2(2)	−0.6(2)	0.0(2)
C(10)	0.7358(5)	0.2929(5)	0.869(2)	1.4(2)	2.0(2)	2.2(3)	1.0(2)	−0.2(2)	0.6(2)
C(11)	0.4254(5)	0.2781(5)	0.350(2)	1.3(2)	2.0(2)	1.7(3)	0.9(2)	−0.4(2)	0.1(2)
C(12)	0.4151(5)	0.3513(5)	0.218(2)	1.6(2)	2.0(2)	3.1(3)	0.8(2)	−0.6(2)	0.3(2)
C(13)	0.3067(5)	0.3356(5)	0.051(2)	1.7(2)	1.8(2)	4.0(4)	1.1(2)	−1.1(2)	0.2(3)
C(14)	0.2058(5)	0.2459(5)	0.040(2)	1.5(2)	2.2(2)	3.2(3)	1.2(2)	−1.0(2)	−0.1(3)
C(15)	0.2146(5)	0.1723(5)	0.166(2)	1.4(2)	1.9(2)	2.7(3)	0.8(2)	−0.4(2)	0.2(2)
C(16)	0.3241(5)	0.1880(5)	0.326(2)	2.0(2)	1.8(2)	2.6(3)	1.3(2)	−0.6(2)	0.0(2)
O(18)	0.9354(4)	0.3666(3)	1.171(2)	1.7(1)	1.9(2)	6.1(3)	0.4(2)	−2.0(2)	0.3(2)
O(19)	0.6916(4)	0.0337(4)	1.075(2)	2.5(1)	1.9(2)	6.6(4)	1.2(2)	−1.6(2)	0.3(2)
O(20)	0.6541(4)	0.4605(3)	0.539(2)	2.0(1)	1.7(2)	4.5(3)	0.8(2)	−1.2(2)	0.4(2)
O(22)	0.1129(4)	0.0849(3)	0.142(2)	1.6(1)	1.7(2)	6.5(3)	0.5(2)	−1.6(2)	0.3(2)
O(1)	0.5318(3)	0.2111(3)	0.603(2)	1.6(1)	1.6(1)	2.7(2)	1.0(2)	−1.1(1)	0.1(2)
O(4)	0.8427(4)	0.4586(3)	0.888(2)	1.6(1)	1.7(2)	5.0(3)	0.6(2)	−1.5(2)	−0.3(2)
O(21)	0.0952(3)	0.2271(3)	−0.123(2)	1.2(1)	2.1(2)	5.3(3)	0.8(2)	−1.7(2)	0.0(2)
O(W1)	0.0925(4)	−0.0602(4)	0.528(2)	2.9(1)	2.8(2)	4.3(3)	2.0(2)	−1.2(2)	−0.1(2)
O(W2)	0.1225(4)	0.3893(4)	−0.366(2)	2.4(1)	2.7(2)	3.6(3)	1.6(2)	−1.1(2)	0.3(2)
H(6)	0.885	0.197	1.248	4.0					
H(8)	0.530	0.062	0.756	2.4					
H(12)	0.487	0.417	0.246	4.0					
H(13)	0.301	0.388	−0.059	4.0					
H(16)	0.331	0.135	0.421	4.0					
H(20)	0.732	0.505	0.526	5.0					
H(19)	0.747	0.037	1.252	5.0					
H(18)	0.938	0.408	1.001	5.0					
H(21)	0.114	0.288	−0.200	5.0					
H(22)	0.123	0.040	0.289	5.0					

Note. Positional parameters are listed as fractions of cell edges. Anisotropic temperature factors are expressed as $\exp[-\frac{1}{4}(h^2a^{*2}B_{11} + k^2b^{*2}B_{22} + l^2c^{*2}B_{33} + 2hka^*b^*B_{12} + 2hla^*c^*B_{13} + 2klb^*c^*B_{23})]$ and isotropic temperature factors are listed as $\exp(-B \sin^2\theta/\lambda^2)$ with B values given in Å^2. Estimated standard deviations, with respect to the last digit listed, are given in parentheses.

atomic scattering factors used for carbon and oxygen atoms (*38*) and for hydrogen atoms (*39*) are listed in the literature. Final positional and thermal parameters are listed in Table 2. Lists of calculated and observed structure factors are available.[2]

[2] Supplementary material (lists of calculated and observed structure factors) are available from Dr. Miriam Rossi, Department of Chemistry, Vassar College, Poughkeepsie, N.Y. 12601.

RESULTS AND DISCUSSION

Description of the Structure

Crystal data are collected in Table 1. The structural parameters and conformation of quercetin are presented in Fig. 1 and Table 2. Intramolecular bond distances, bond angles, and torsion angles are listed in Tables 3, 4, and 5. These values are comparable with those found for similar compounds, such as 7,8-benzoflavone and 5,6-benzoflavone (*15*). The major difference is the C4–C10 bond length. In quercetin, this bond length is 1.418(8) Å, while for 7,8-benzoflavone it is 1.477(5) Å and for 5,6-benzoflavone it is 1.460(4) Å. This short distance seems to reflect the strong intramolecular hydrogen bond O18–H18 . . . O4 [2.586(5) Å] which forms a stable six-membered "ring." This ring is planar (rms deviation from the plane defined by the atoms is 0.0138).

The main result derived from this structure determination which is manifest in Fig. 1 is that quercetin exists in a fairly planar conformation. The twist of the exocyclic phenyl ring relative to the rest of the molecule as characterized by the C2–C11 torsion angle is 7°. The conformation of the hydroxyl groups is, as expected, such that the hydrogen atoms are located to maximize hydrogen bonding. Stacking interactions along z between translationally related molecules are evident, as expected from the value of the c unit cell constant. These and van der Waals interactions provide the other cohesive forces in the crystal packing arrangement. A stereo view of the unit cell is given in Fig. 2.

Quercetin has primarily hydrogen bond donors—with five hydroxyl groups. Two of these hydroxyl groups, O18 and O20, are involved in intramolecular

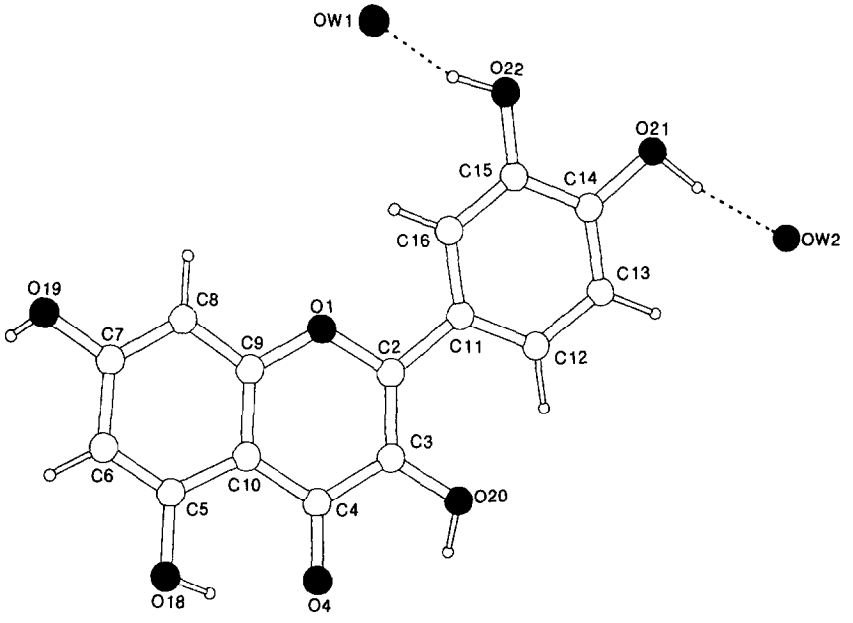

FIG. 1. Molecular structure of quercetin utilizing the nomenclature scheme from the text. View of the best plane of the molecule. The twist about the C2–C11 bond is 7°.

TABLE 3

BOND LENGTHS FOR QUERCETIN

Bond	Length (Å)	Bond	Length (Å)
O1–C2	1.365(7)	C5–C6	1.355(8)
O1–C9	1.370(4)	C5–C10	1.420(6)
O4–C4	1.267(7)	C6–C7	1.403(8)
O18–C5	1.375(7)	C6–H6	1.006(4)
O18–H18	0.948(5)	C7–C8	1.386(6)
O19–C7	1.358(7)	C8–C9	1.397(8)
O19–H19	0.914(5)	C8–H8	1.022(6)
O20–C3	1.351(7)	C9–C10	1.392(8)
O20–H20	0.906(3)	C11–C12	1.388(8)
O21–C14	1.396(5)	C11–C16	1.397(8)
O21–H21	0.975(4)	C12–C13	1.391(6)
O22–C15	1.373(7)	C12–H12	1.005(6)
O22–H22	0.990(5)	C13–C14	1.393(8)
C2–C3	1.357(8)	C13–H13	1.008(6)
C2–C11	1.479(5)	C14–C15	1.376(8)
C3–C4	1.449(6)	C15–C16	1.396(5)
C4–C10	1.418(8)	C16–H16	1.006(6)

TABLE 4

BOND ANGLES FOR QUERCETIN

Bond	Angle (°)	Bond	Angle (°)
C2–O1–C9	120.90(4)	C8–C9–C10	122.79(4)
C5–O18–H18	101.93(5)	C8–C9–O1	116.79(4)
C7–O19–H19	113.42(5)	C10–C9–O1	120.42(5)
C3–O20–H20	110.29(2)	C4–C10–C5	122.83(5)
C14–O21–H21	101.87(4)	C4–C10–C9	120.17(4)
C15–O22–H22	112.59(4)	C5–C10–C9	116.96(5)
C3–C2–C11	127.75(5)	C2–C11–C12	121.34(5)
C3–C2–O1	121.26(3)	C2–C11–C16	119.34(5)
C11–C2–O1	110.97(4)	C12–C11–C16	119.30(4)
C2–C3–C4	120.33(5)	C11–C12–C13	121.02(5)
C2–C3–O20	122.25(4)	C11–C12–H12	119.35(4)
C4–C3–O20	117.34(5)	C13–C12–H12	119.62(5)
C3–C4–C10	116.79(5)	C12–C13–C14	118.84(5)
C3–C4–O4	120.33(5)	C12–C13–H13	120.76(5)
C10–C4–O4	122.82(4)	C14–C13–H13	120.39(4)
C6–C5–C10	122.14(5)	C13–C14–C15	120.78(4)
C6–C5–O18	119.37(4)	C13–C14–O21	120.73(5)
C10–C5–O18	118.45(5)	C15–C14–O21	118.33(5)
C5–C6–C7	118.62(4)	C14–C15–C16	120.04(5)
C5–C6–H6	120.95(6)	C14–C15–O22	118.52(3)
C7–C6–H6	120.44(6)	C16–C15–O22	121.40(5)
C6–C7–C8	122.36(5)	C11–C16–C15	119.83(5)
C6–C7–O19	119.84(4)	C11–C16–H16	119.47(4)
C8–C7–O19	117.66(5)	C15–C16–H16	120.70(5)
C7–C8–C9	117.08(5)		
C7–C8–H8	122.71(5)		
C9–C8–H8	120.22(4)		

TABLE 5

TORSION ANGLES (DEGREES) FOR QUERCETIN

O1–C2–C11–C16	7(1)
C3–C2–C11–C12	7(1)
C6–C7–O19–H19	17(1)
C6–C5–O18–H18	152(1)
C4–C3–O20–H20	26(1)
C13–C14–O21–H21	−1(1)
C16–C15–O22–H22	11(1)

hydrogen bonding with the only hydrogen bond acceptor on the molecule itself, the exocyclic oxygen, O4. The other three, O22, O21, and O19, participate in intermolecular hydrogen bonding interactions with the two solvent waters of crystallization.

The structure can be described as layers of hydrogen bond dimers that pack almost perpendicular to the *c* axis. Hydrogen bonds between the exocyclic oxygen, O4, and the hydroxyl group, O18, of an inversion related molecule make up the dimers. These dimers form a two-dimensional net mainly in the *ab* plane connected through the hydrogen bonding network of the solvent water molecules. The waters, OW1 and OW2, join these layers in the *z* direction. There are chains of O22 . . . OW1 . . . O22 and O4 . . . OW2 . . . O4 where the two quercetin molecules are related by a unit cell translation in *z*. Hydrogen bond parameters are given in Table 6.

Notable is the preponderance of attractive forces involving the exocyclic oxygen, O4. It appears to be a focal point of cohesive forces in the crystal structure. The electron-withdrawing capacity of O4 is demonstrated using resonance.

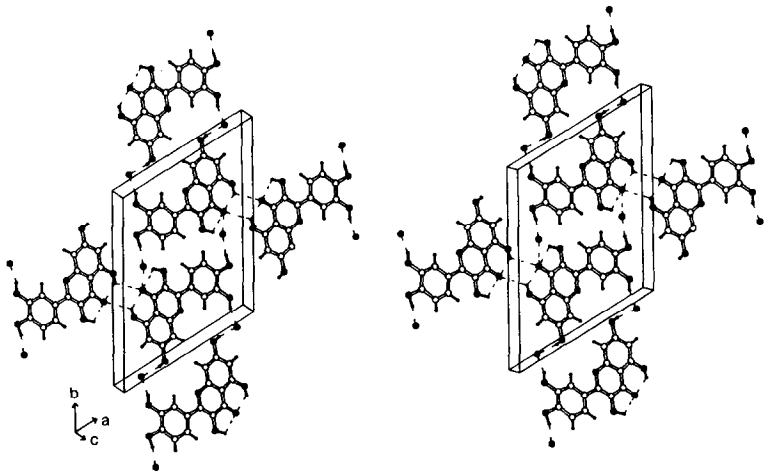

FIG. 2. A stereo view of the unit cell in which the planarity and intermolecular forces inherent in the crystal structure are seen.

TABLE 6

HYDROGEN BOND PARAMETERS FOR QUERCETIN

D — H --- A	Acceptor (A)	D---A	H—D	H---A	A--H—D
O18 —H18---O4	x, y, z	2.586(4)	0.948(5)	1.841(3)	133.5(2)
O20 —H20---O4	x, y, z	2.712(4)	0.906(3)	2.323(4)	105.7(2)
O20 —H20---OW2	$1-x, 1-y, -z$	2.853(5)	0.906(3)	1.979(4)	161.6(2)
O21 —H21---OW2	x, y, z	2.722(6)	0.975(4)	1.757(4)	170.0(2)
O22 —H22---OW1	x, y, z	2.750(7)	0.990(5)	1.792(5)	162.0(2)
OW1— ---O21	$-x, -y, -z$	2.860(7)			
OW1— ---O22	$x, y, 1+z$	3.153(7)			
OW1— ---O22	$-x, -y, -z$	3.373(6)			
OW1— ---O22	$-x, -y, 1-z$	2.880(4)			
OW2— ---O4	$1-x, 1-y, -z$	3.107(7)			
OW2— ---O4	$1-x, 1-y, 1-z$	2.849(7)			
OW2— ---O18	$-1+x, y, -1+z$	3.159(6)			

Resonance forms depicting the phenyl and pyrone portions of the skeleton flavone structure are shown in Scheme 2 (**III** and **IV**). Inspection of the flavonoid skeleton structure conformational energy analysis reveals that a minimum potential energy configuration exists at a torsion angle of 22.8° about the C2–C11 bond (*15*). This represents a compromise between two effects: repulsive steric hindrance between atoms and attractive forces due to more extensive conjugation. Ideally, the phenyl ring would exist at a conformation perpendicular to the pyrone ring, to minimize steric hindrance between atoms. However, in order to maximize the positive contribution from a conjugated electron system, the two rings should be planar. At a calculated zero torsion angle about the C2–C11 bond, the energy is 0.7 kcal/mol above the minimum energy value. Thus, if there are forces present which can stabilize the negative charge on O4, the more planar configuration is expected; otherwise the lower energy nonplanar form predominates. Structural analysis of quercetin has revealed a number of hydrogen bonding interactions in which it is an acceptor, thus stabilizing the negative charge on O4.

X-Ray analysis of other flavonoid structures demonstrates the importance of this property. These are shown in Fig. 3. 7,8-Benzoflavone is nonplanar, having a 22° torsion angle between the phenyl ring and the pyrone portion. There are no

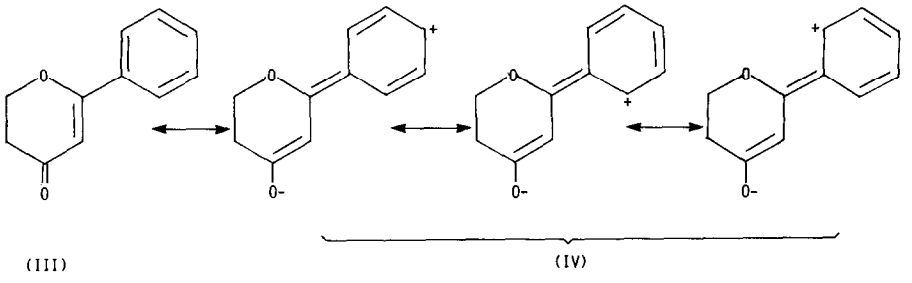

(III) (IV)

SCHEME 2.

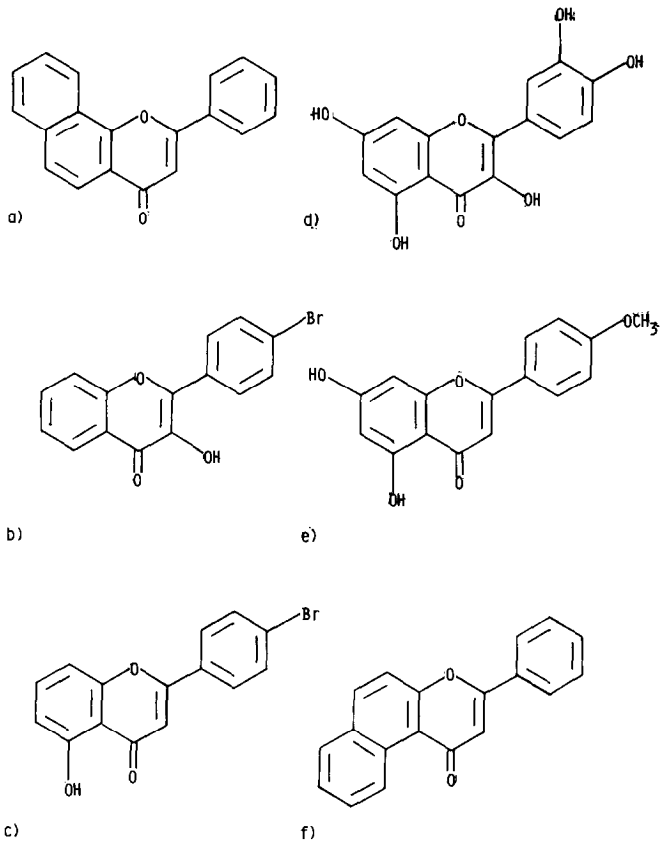

FIG. 3. Other flavonoid structures that have been investigated crystallographically. In parentheses are the values of the C2–C11 torsion angle (t). (a) 7,8-Benzoflavone [t = 23.8(2)°]; (b) 4′-Br-3-OH flavone (t = 18.8°); (c) 4′-Br-5-OH flavone (t = 6.6°); (d) quercetin [t = 7.0(1.0)°]; (e) acacetin (t = 3.1°); (f) 5,6-benzoflavone [t = −1.0(3)°].

solvent molecules and, therefore, only weak van der Waals interactions between molecules in the unit cell account for its conformation and crystal packing. The major contribution to its conformation is from the resonance form (**III**). Likewise, 4′-bromo-3-hydroxyflavone (*40*) displays no hydrogen bond formation in the crystalline state and its torsion angle is 18.8°, indicating that the major influence in its conformation is the minimization of steric effects. 5,6-Benzoflavone, conversely, is planar (torsion angle is −1.0°) and crystallizes with a solvent water molecule. It is hydrogen bonded to the negatively charged acceptor, O4, thus eliciting greater contribution from resonance form **IV**. 4′-Bromo-5-hydroxyflavone (*40*) has a 6.6° torsion angle (fairly planar) and an intramolecular hydrogen bond between the 5-hydroxyl group and the carbonyl oxygen. Similarly, acacetin, (*41*) has a small torsion angle (3.1°) due to an intramolecular hydrogen bond from the same two exocyclic groups.

In summary, planar conformations of flavonoid structures exist when stabilization of the negative charge on the exocyclic oxygen is possible. Stabilization

occurs in known crystal structures through hydrogen bonding. These interactions are strong enough to overcome the small potential energy barrier and permit the molecule to achieve planarity.

Enzyme Inhibition

Because of quercetin's interactions with many enzyme systems, what is known about its activity is very vague. It has a remarkable affinity for membranes and membrane-bound enzymes (*42*). These include the metabolizing cytochrome *P*-450 enzymes, transport nucleoside triphosphatases, aldose reductase, and cyclic nucleotide phosphodiesterases. Additionally, other proteins involved with ion transport across membranes are inhibited by quercetin. It is known that quercetin causes conformational changes in the enzymes (*43*). Previously, it was believed that quercetin acts on amino and sulfhydryl groups on the enzymes; recent studies have contradicted this. Quercetin was shown not to bind covalently to functional

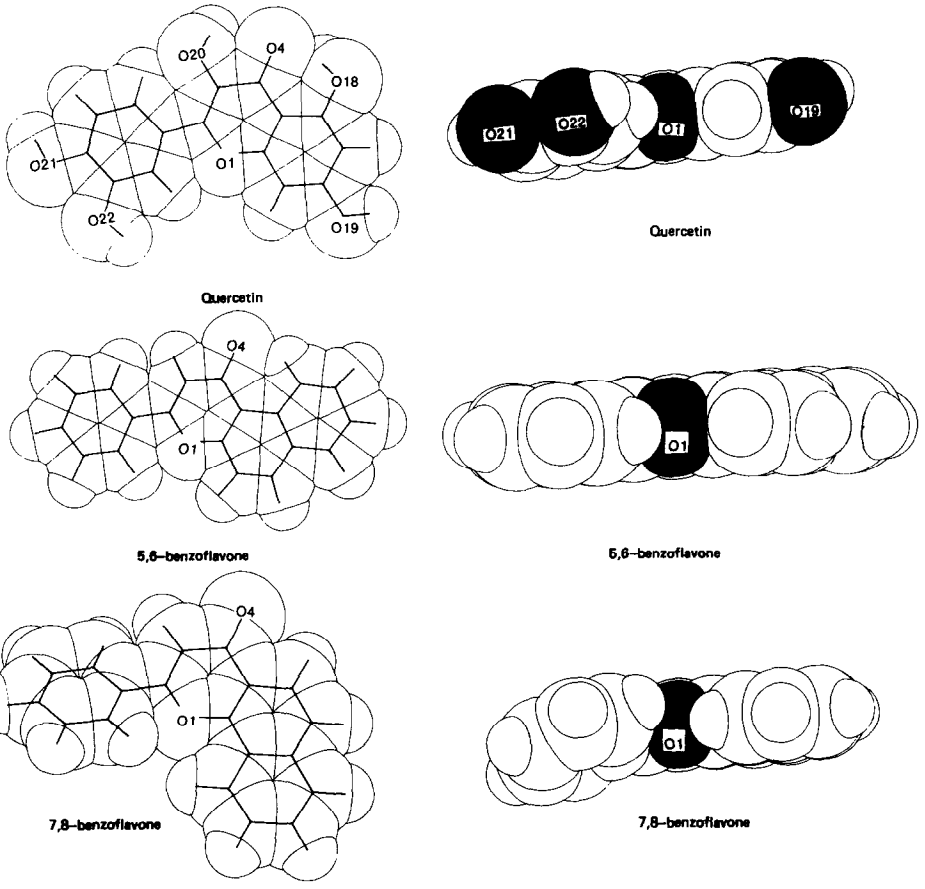

FIG. 4. Molecular shape of quercetin, 5,6-benzoflavone, and 7,8-benzoflavone. The two views are looking at the best plane of the molecules and along the O1–O4 direction in the pyrone ring.

groups on the protein responsible for phosphorylation (*44*), although it does interact with the membrane. In its role as an anti-inflammatory agent, quercetin inhibits activation of leukocyte respiration through interactions at the membrane at a hydrophobic site on the protein (*29*). It was suggested that quercetin inhibits cyclic nucleotide phosphodiesterase by mimicking the pyrimidine ring (with its pyrone ring) used in stacking interactions between the base and the protein (*4*). In its role as a hyaluronidase inhibitor, it was shown to be capable of orthoquinone formation (*35*). This is of interest because quinones are known to divert electron flow from the enzymatic cycle in electron transfer reactions, many of which are inhibited by quercetin.

Quinones, as well as flavones, are direct-acting reversible inhibitors of cytochrome *P*-450. Testa and Jenner (*2*) have analyzed the properties of *P*-450 inhibitors and determined that almost all have available a direct-acting or metabolically activated functional group capable of binding to *P*-450. Such binding can prevent either of two steps in the catalytic cycle: the reduction of *P*-450 via NADPH cytochrome *P*-450 reductase and/or binding of molecular oxygen. From the crystal structure determination of quercetin, as with other flavonoid inhibitors of *P*-450 (*15*), it is seen that the exocyclic oxygen plays a pivotal role in the molecular structure. It has also been reported that quercetin inhibits the NADPH cytochrome *P*-450 reductase involved in the metabolism of benzo[*a*]pyrene and aflatoxin B1 (*16, 45*). Inactivation of bay region diol epoxides by quercetin was due to its direct, covalent interaction with these diol epoxides (*17*), rather than on the cells. The phenolic groups of quercetin are important for this since flavonoids

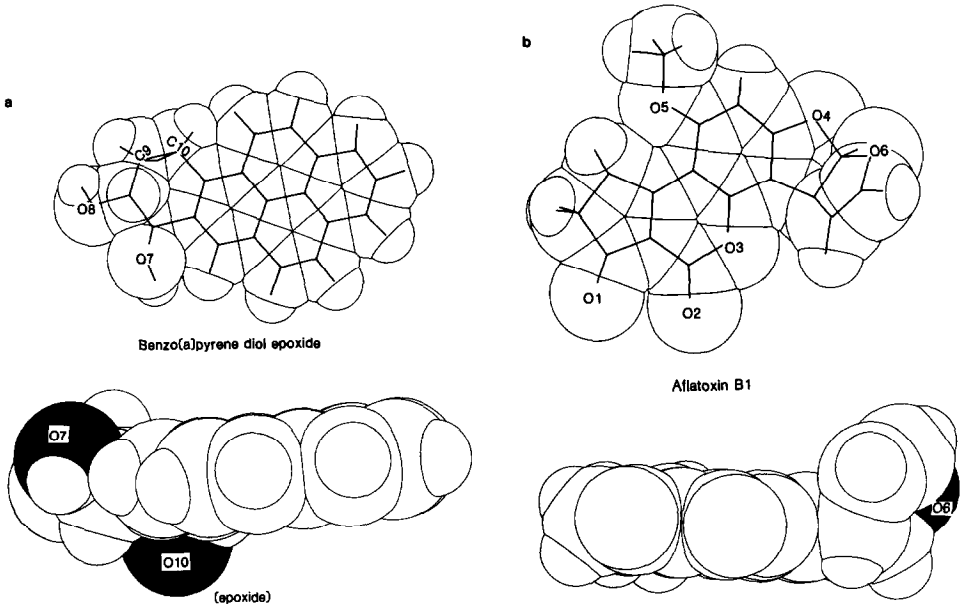

FIG. 5. Molecular shape of (a) benzo[*a*]pyrene and (b) aflatoxin B1. Again, the two views are the best plane of the molecules and perpendicular to it.

which lacked free phenolic groups were inactive. Although not characterized, a similar covalent interaction led to an inactive complex between the phenolic plant compound, ellagic acid, and the benzo[*a*]pyrene diol epoxide (*46*). To be a competitive inhibitor, quercetin must be able to mimic the activity of substrates to the protein. The similarity in shape between flavones and the polycyclic aromatic hydrocarbons they inhibit has been discussed (*15*). In Fig. 4 are shown the molecular shapes of quercetin and other flavonoid inhibitors of cytochrome *P*-450, and in Fig. 5, the carcinogenic substrates (benzo[*a*]pyrene and aflatoxin B1) whose activity is curtailed by quercetin. These diagrams of the molecular surfaces are obtained from summing the van der Waals radii of the constituent atoms. They were produced using the computer program CHEMGRAF (*47*).

A detailed analysis of pharmacophor requirements for aldose reductase (*31*) has been published. From structure–activity relationships of inhibitors of the enzyme, the authors developed a model of the active site. Quercetin was included in this study and it was determined that its activity toward aldose reductase results partly from its aromatic ring next to the pyrone ring. The nucleophilic carbonyl group was found to be of importance in bonding to the inhibitor site through a postulated

TABLE 7

NET ATOMIC CHARGES FOR FLAVONOIDS

	Quercetin		7,8-Benzoflavone	5,6-Benzoflavone
O1	−0.2444		−0.2519	−0.2066
O4	−0.4063		−0.3739	−0.3366
C2	0.1667		0.2525	0.2095
C3	0.0630		−0.1634	−0.1494
C4	0.3046		0.3336	0.2679
C5	0.2977		0.0618	0.0514
C6	−0.1636		−0.0223	0.0057
C7	0.2988		0.0536	0.0277
C8	−0.1556		−0.0243	−0.0541
C9	0.2787		0.2225	0.1944
C10	−0.1945		−0.1094	−0.0995
C11	0.0146		−0.0077	0.0014
C12	0.0133		0.0279	0.0192
C13	−0.0340		0.0226	0.0060
C14	0.1637		0.0209	0.0159
C15	0.1756		0.0197	0.0042
C16	−0.0394		0.0328	0.0158
O18	−0.3214			
O19	−0.3076			
O20	−0.2895			
O21	−0.2860			
O22	−0.2861			
		C17	0.0310	−0.0264
		C18	0.0317	0.0199
		C19	0.0346	−0.0060
		C20	0.0045	0.0030

charge-transfer mechanism. The hydroxyl groups provided enhanced binding through their hydrogen bonding capacity.

The electronic properties of quercetin have been calculated since any interactions with proteins must be governed by both electronic and steric factors. The net charges calculated using CNDO/2 (*48*) for the experimentally determined atomic parameters are listed in Table 7. These charges are compared to those obtained for other flavone inhibitors of cytochrome *P*-450 in the same table. It is clear that while quercetin has more polar groups than either 5,6- or 7,8-benzoflavone, all three share a nucleophilic carbonyl group which could be used for binding. Similar analyses for aldose reductase inhibitors revealed the presence of these negatively charged carbonyl groups in active compounds.

Tapping the information gained from the structural and electronic studies of quercetin is important because of its varied activities in the body and its ubiquitous nature in our food supply. It is of interest to develop more specific drugs which act on these activities. Drug design using this method has produced some success in other systems. Work in this area is in progress in an attempt to establish the criteria necessary for the inhibition of many of these enzymes.

ACKNOWLEDGMENTS

This research was supported by National Science Foundation Grant R11-8300122 (to M.R.) and National Institutes of Health Grants CA-10925 and CA-22780 which were awarded to Dr. Jenny P. Glusker and The Institute for Cancer Research (ICR), where the diffractometer data were collected and graphics work done. I am especially grateful to Dr. Jenny P. Glusker for her constant support and encouragement, and to Dr. Peter Murray-Rust, the members of the crystallographic laboratories at ICR, and Dr. Vivian Cody for helpful conversations.

REFERENCES

1. Brown, J. P. (1980) *Mutat. Res.* **75,** 243–277.
2. Testa, B., and Jenner, P. (1981) *Drug Metab. Rev.* **12,** 1–117.
3. Yoshimoto, T., Furukawa, M., Yamamoto, S., Horie, T., and Watanabe-Kohno, S. (1983) *Biochem. Biophys. Res. Commun.* **116,** 612–618.
4. Picq, M., Prigent, A. F., Nemoz, G., Andre, A. C., and Pacheco, H. (1982) *J. Med. Chem.* **25,** 1192–1198.
5. Gschwendt, M., Horn, F., Kittstein, W., and Marks, F. (1983) *Biochem. Biophys. Res. Commun.* **117,** 444–447.
6. Kato, R., Nakadate, T. Yamamoto, S., and Sugimura, T. (1983) *Carcinogenesis* **4,** 1301–1305.
7. Kuriki, Y., and Racker, E. (1976) *Biochemistry* **15,** 4951–4956.
8. Shoshan, V., and MacLennan, D. H. (1981) *J. Biol. Chem.* **256,** 887–892.
9. Varma, S. D., and Kinoshita, J. H. (1976) *Biochem. Pharmacol.* **25,** 2505–2513.
10. Ferrell, J. E., Chang-Sing, P. D. G. Loew, G., King, R., Mansour, J. M., and Mansour, T. E. (1979) *Mol. Pharmacol.* **16,** 556–568.
11. Booth, A. N., Murray, C. W., Jones, F. T., and DeEds, F. (1956) *J. Biol. Chem.* **223,** 251–257.
12. Stoewsand, G. S., Hrazdina, G., Babish, J. C., and Walsh, K. M. (1984) *Fed. Proc.* **43,** 688.
13. Pamuckcu, A. M., Yalciner, S., Hatcher, J. F., and Bryan, G. T. (1980) *Cancer Res.* **40,** 3468–3472.

14. LU, A. Y. H., AND WEST, S. B. (1980) *Pharmacol. Rev.* **31,** 277.
15. ROSSI, M., CANTRELL, J. S. FARBER, A. J., DYOTT, T. CARRELL, H. L., AND GLUSKER, J. P. (1980) *Cancer Res.* **40,** 2774–2784.
16. BUENING, M. K., CHANG, R. L., HUANG, M-T., FORTNER, J. G., WOOD, A. W., AND CONNEY, A. H. (1981) *Cancer Res.* **41,** 67–72.
17. HUANG, M-T., WOOD, A. W., NEWMARK, H. L., SAYER, J. M., YAGI, H., JERINA, D. M., AND CONNEY, A. H. (1983) *Carcinogenesis* **4,** 1631–1637.
18. SUOLINNA, E-M., BUCHSBAUM, R. N., AND RACKER, E. (1975) *Cancer Res.* **35,** 1865–1872.
19. LANG, D. R., AND RACKER, E. (1974) *Biochim. Biophys. Acta* **333,** 180–186.
20. KIM, J. H., KIM, S. H., ALFIERI, A. A., AND YOUNG, C. W. (1984) *Cancer Res.* **44,** 102–106.
21. BELT, J. A., THOMAS, J. A., BUCHSBAUM, R. N., AND RACKER, E. (1979) *Biochemistry* **18,** 3506.
22. GRAZIANI, Y., CHAYOTH, R., KARNY, N., FELDMAN, B., AND LEVY, J. (1981) *Biochim. Biophys. Acta* **714,** 415–421.
23. MIDDLETON, E., JR., AND DRZEWIECKI, G. (1984) *Biochem. Pharmacol.* **33,** 3333–3338.
24. FEWTRELL, C. M. S., AND GOMPERTS, B. D. (1977) *Nature (London)* **265,** 635–636.
25. SOSHAN, V., CAMPBELL, K. P., MACLENNAN, D. H., FRODIS, W., AND BRITT, B. A. (1980) *Proc. Natl. Acad. Sci. USA* **77,** 4435–4438.
26. SARKADI, B., SZASZ, I., AND GARDOS, G. (1980) *Biochim. Biophys. Acta* **598,** 326.
27. NISHINO, H., NAITOH, E., IWASHIMA, A., AND UMEZAWA, K. (1984) *Experientia* **40,** 184–185.
28. BERETZ, A., STIERLE, A., ANTON, R., AND CAZENAVE, J-P. (1981) *Biochem. Pharmacol.* **31,** 3597–3600.
29. BERTON, G., SCHNEIDER, C., AND ROMEO, D. (1980) *Biochim. Biophys. Acta* **595,** 47–55.
30. MOORE, P. K., GRIFFITHS, R. J., AND LOFTS, F. J. (1983) *Biochem. Pharmacol.* **32,** 2813–2817.
31. KADOR, P. F., AND SHARPLESS, N. E. (1983) *Mol. Pharmacol.* **24,** 521–531.
32. KUHNAU, J. (1976) *World Rev. Nutr. Diet* **24,** 117–191.
33. PRATT, D. E., AND WATTS, B. M. (1964) *J. Food Sci.* **29,** 27–33.
34. NOSE, K. (1984) *Biochem. Pharmacol.* **33,** 3823–3827.
35. RODNEY, G., SWANSON, A. L., WHEELER, L. M., SMITH, G. N., AND WORREL, C. S. (1950) *J. Biol. Chem.* **183,** 739–747.
36. SHELDRICK, G. M. (1976) SHELX76. Program for Crystal Structure Determination, University of Cambridge, England.
37. CARRELL, H. L., SHIEH, H. S., TAKUSAGAWA, F., AND WOOD, W. P. (1978) Crystallographic Programs from The Institute for Cancer Research, Inst. for Cancer Res., Philadelphia.
38. CROMER, D. T., AND WABER, J. T. (1965) *Acta Crystallogr* **18,** 104–109.
39. STEWART, R. F., DAVIDSON, E. R., AND SIMPSON, W. T. (1965) *J. Chem. Phys.* **42,** 3175–3187.
40. HAYASHI, T., KAWAI, S., OHNO, T., IITAKA, Y., AND AKIMOTO, T. (1974) *Chem. Pharm. Bull.* **22,** 1212.
41. CANTRELL, J. S., AND GERDOM, S. (1979) unpublished results.
42. CARPENEDO, F. BORTIGNON, C., BRUNI, A., AND SANTI, R. (1969) *Biochem. Pharmacol.* **18,** 1495–1500.
43. CANTLEY, L. C., JR., AND HAMMES, G. C. (1976) *Biochemistry* **15,** 1–8.
44. SHOSHAN, V., SHAHAK, Y., AND SHAVIT, N. (1980) *Biochim. Biophys. Acta* **591,** 421–433.
45. NIXON, J. E. HENDRICKS, J. D., PAWLOWSKI, N. E., PEREIRA, C. B., SINNHUBER, R. O., AND BAILEY, G. S. (1984) *Carcinogenesis* **5,** 615–619.
46. SAYER, J. M., YAGI, H., WOOD, A. W., CONNEY, A. H., AND JERINA, D. M. (1982) *J. Amer. Chem. Soc.* **104,** 5562.
47. CHEMGRAF (1984) Graphics Program, Chemical Design, Ltd., Oxford.
48. POPLE, J. A., AND BEVERIDGE, D. L. (1970) Approximate Molecular Orbital Theory, pp. 163–193, Appendix A, McGraw–Hill, New York.